



Phase separation in solvent extraction of cobalt from acidic sulfate solution using synergistic mixture containing dinonylnaphthalene sulfonic acid and 2-ethylhexyl 4-pyridinecarboxylate ester

Ting HUANG, Yong-xi WANG, Hui-ping HU, Fang HU, Yu-qing LUO, Shi-jun LIU

College of Chemistry and Chemical Engineering, Central South University, Changsha 410083, China

Received 26 February 2018; accepted 4 March 2019

Abstract: Phase separation rate is a critical character in determining the usefulness of a solvent extraction system in hydrometallurgy. A survey of the synergistic mixture containing dinonylnaphthalene sulfonic acid (HDNNS) and 2-ethylhexyl 4-pyridinecarboxylate ester (4PC) for the extraction of cobalt from acidic single metal sulfate solution was carried out to suggest how the physicochemical properties and the morphology of the reverse micelles in the loaded organic phase affect the phase separation. The results show that effective parameters affecting the phase separation are the viscosity and the excess water uptake of the loaded organic phase. It is obvious that the specific settling rate (SSR) decreases with the apparent increase of these two parameters. The measurement of small angle X-ray scattering (SAXS) proves that the morphology of the reversed micelles in the loaded organic phase changes evidently with the change of the specific settling rate (SSR).

Key words: synergistic solvent extraction; phase separation; specific settling rate; reverse micelle; cobalt

1 Introduction

Solvent extraction (SX) of metal ions has been widely used in hydrometallurgical separation processes for many years [1]. Synergistic solvent extraction (SSX) has also attracted considerable attention because it has higher extraction efficiency and selectivity for the target metals than solvent extraction (SX), and many SSX systems have been developed in the past three decades [2]. In the 1990s, PRESTON and du PREEZ [3] claimed that the synergistic mixture containing dinonylnaphthalene sulfonic acid (HDNNS) and 2-ethylhexyl 4-pyridinecarboxylate ester (4PC) has the ability to selectively extract copper, nickel and cobalt from acidic multi-metal sulfate solutions with impurities such as iron, aluminum, manganese, magnesium and calcium. However, this synergistic extraction system has lower specific setting rate of phase separation, which is a major drawback in terms of industrial process implementation [4]. Our preliminary study indicated that 4PC has no ability to extract metal ions, but the mixture

system of HDNNS and 4PC can extract Cu(II), Ni(II), and Co(II) from acidic multi-metal sulfate solutions with about pH 2, and the extraction efficiency of copper is higher than that of other metal ions [5]. Moreover, previous laboratory-scale experiment in our group [6] showed that the specific setting rate of the synergistic mixture containing 0.25 mol/L HDNNS and 0.5 mol/L 4PC for the extraction of nickel from multi-metal acidic sulfate solutions is less than $2.0 \text{ m}^3/(\text{m}^2 \cdot \text{h})$, which is lower than admissible value on mixer-settler ($\geq 2.4 \text{ m}^3/(\text{m}^2 \cdot \text{h})$) [7]. To improve this SSX technique, it is necessary to find the factors that will affect the phase separation behavior.

The phase separation process is complex and extremely difficult to be analyzed because numerous factors can affect the phase separation behavior. As a complex interfacial process, it is related to the geometrical parameters of the mixer-settler [8,9], the hydromechanics conditions [10,11], the physicochemical properties of extraction system (density, viscosity and interfacial tension) [12–15], the structure of extractants and extractive compound [16,17], and the probable

Foundation item: Project (2014CB643401) supported by the National Basic Research Program of China; Project (51674294) supported by the National Natural Science Foundation of China; Project (2016TP1007) supported by the Hunan Provincial Science and Technology Plan, China

Corresponding author: Shi-jun LIU, Tel: +86-13875951963, E-mail: shijunliu@csu.edu.cn;

Hui-ping HU, Tel: +86-18107487664, E-mail: phuhuiping@126.com

DOI: 10.1016/S1003-6326(19)65019-3

formation of the reversed micelles in the loaded organic phase [18–20]. It is not yet known what are the main factors affecting the phase separation behavior.

Some researches tried to understand the effect of physicochemical properties of the extraction system on the phase disengagement rate. In the system of copper solvent extraction, LIU et al [13] found that with the increase of Lix984N content, the phase disengagement rate and the interfacial tension decreased, and the density and the viscosity of the loaded organic phase slightly increased. They [14] also found that with the increase of contact time between the organic phase and aqueous acidic phase, the phase disengagement rate decreased rapidly and the density and viscosity of the loaded organic phase decreased slightly. In the solvent extraction of Amex uranium with tertiary amine extractants, MOVER and McDOWELL [17] found that the phase disengagement time and the interfacial tension increases with increasing alkyl chain length of amine and that the phase disengagement time increases as the interfacial tension increases. This result is opposite to the effect expected from reasoning that higher interfacial tension indicates greater thermodynamic instability toward breaking and therefore causes a decrease in phase disengagement time. In fact, the interfacial tension is not by itself a reliable measure for the prediction of phase disengagement rates [21].

In general, it is well known that the physicochemical properties of the system depend on its structure. Therefore, the most important factor affecting the phase separation behavior should be the structure of the system, including the structure of metal ions in aqueous phase and the structure of extractant and metal extracts in organic phase. A coordination extraction complex in Co(II) extraction system containing HDNNS and 4PC was prepared [22], and the results show that the structure of the extraction complex is formed by the coordination of Co(II) with four water molecules and two 4PC molecules. HDNNS molecule did not enter into the structure of cobalt extract compound, but it should affect the phase disengagement rates.

Therefore, in the present work, the phase separation behavior between the acidic sulfate aqueous phase containing Co(II) and the organic phase of the synergistic mixture containing HDNNS and 4PC was investigated to suggest the effects of physicochemical properties and the morphology of the reversed micelles in the loaded organic phase on the phase separation behavior. The physicochemical parameters in terms of changes in the density, viscosity, interfacial tension and specific settling rate (SSR) were measured when the concentration of extractant changed. The measurement of small angle X-ray scattering (SAXS) was used to identify the morphology of the reversed micelles in the

loaded organic phase.

2 Experimental

2.1 Chemical materials

Dinonylnaphthalene sulfonic acid, HDNNS, supplied by Shanghai Jia Chen Chemical Co. Ltd., was purified and verified according to our previous study [23]. 2-ethylhexyl 4-pyridinecarboxylate ester, 4PC, was synthesized following the procedure described elsewhere [24]. Escaid 110 (200–248 °C fraction hydrocarbon fluid with 99.5% aliphatic content) and n-dodecane (99%) were correspondingly supplied by ExxonMobil Chemical and Admas-beta, and used as diluents without further purification. All other chemicals were of analytical grade and used without further purification.

2.2 Preparation of aqueous and organic phases

The aqueous feed containing 5 g/L cobalt(II) with 0.5 mol/L Na₂SO₄ supporting electrolyte was used in the present work, the aqueous solution containing 0.5 mol/L Na₂SO₄ was used as the blank system, and the pH values of both aqueous solution were adjusted to about 2 by adding small amount of concentrated H₂SO₄ or NaOH solution. The salts used were CoSO₄·7H₂O and Na₂SO₄.

A lean organic phase was prepared by dissolving weighed quantities of HDNNS and 4PC in Escaid 110 at a constant molar ratio of 1:2 (HDNNS:4PC). For SAXS measurements, the lean organic phases were prepared with the same procedure as mentioned above while Escaid 110 was replaced with n-dodecane. For the measurement of the interfacial tension, the extractant with the highest concentration was prepared by dissolving known masses of the extractants of HDNNS and 4PC in Escaid 110 at a constant molar ratio of 1:2 (HDNNS:4PC), and the remaining organic solutions were made from the concentrated extractant by volume dilution. The extractant concentration of the organic phase or the organic solution containing HDNNS and 4PC was given in term of HDNNS.

2.3 Experimental set-up for phase separation

The experimental set-up for phase separation was illustrated in Fig. 1. The operation method was comparable to that described previously [25]. Prior to the phase separation test, the glass vessel, the lean organic phase and the aqueous feed were first thermally equilibrated by a refrigerated circulating thermostat (Lauda, Alpha 8A, Germany) at (25.0±0.05) °C for 1 h. Then, the aqueous feed (60 mL) was transferred into the graduated jacketed glass vessel (5.5 cm in diameter, 10 cm in height, 200 mL) which was used to clarify the

characteristics of the phase separation behavior fitted with a paddle (1 cm × 3 cm × 1 mm) briefly positioned centrally and 1 cm from the base of the jacketed glass vessel. The aqueous solution was mechanically stirred at 600 r/min by an overhead stirrer (Precision 100, Heidolph MR Hei-Tec, Germany), and vortexing was effectively eliminated whilst the lean organic phase (60 mL) was added rapidly maintaining the temperature at (25.0±0.05) °C. An appropriate amount of NaOH solution was added during the solvent extraction process to keep the equilibrium pH value of about 1.9 (Mettler Toledo FE20 pH meter equipped with ROSS Sure-flow Combination pH probe), followed by an equilibration for 20 min with mechanical stirring so as to ensure the establishment of equilibrium. The two phases were allowed to disengage and the time for the disengagement was determined.

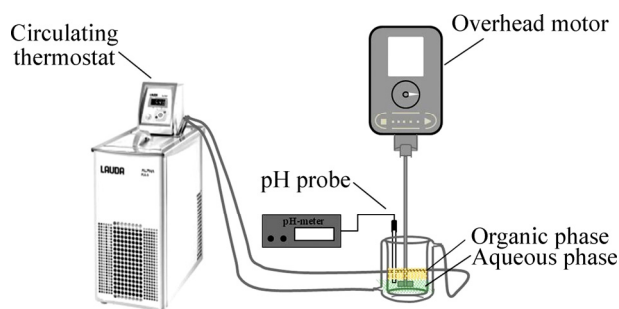


Fig. 1 Experimental set-up for phase separation

In order to determinate quantitatively the rate of the phase separation, the turning time was defined as the time for disappearance of the dispersion band and leaving about half of the interface clear. From the turning time, specific settling rate (SSR, R_{SS}) was calculated using Eq. (1):

$$R_{SS} = \frac{V}{a \cdot t} \quad (1)$$

where V is the total volume of the two phases (m^3); a is the cross section area of jacketed glass vessel (m^2); t is the turning time (h).

After determining of the turning time, the loaded organic phase and aqueous phase were separated, and the loaded organic phase was centrifuged (3000 r/min, 5 min) to remove any residual aqueous phase. The aqueous raffinate and the loaded organic phase were stored for subsequent experiments.

2.4 Determination of physicochemical properties for two phases

The densities for the aqueous raffinate and the loaded organic phases were measured at (25.0±0.1) °C on a DA-100M densimeter (Mettler Toledo, Columbus, Ohio, USA). The interfacial tensions between aqueous

raffinate and the loaded organic phases were measured at (25.0±0.1) °C on a dynamic pendant drop tensiometer (Krüss DSA30S, Hamburg, Germany). The viscosity of the loaded organic phases was measured by a Ubbelohde capillary viscometer in a thermostated bath at (25.0±0.1) °C. The water content of the loaded organic phase was determined using Karl Fischer titrations at room temperature (Mettler V30 Karl Fischer Titrator, Switzerland). The contents of cobalt in aqueous feeds and in raffinate were analyzed using Inductively Coupled Plasma-Atomic Emission Spectrometry (ICP-AES, Optima 5300DV, PerkinElmer Ltd., USA). The concentrations of the corresponding metals in the loaded organic phases were calculated by means of mass balance.

In order to determinate the interfacial tension between the aqueous raffinate and the loaded organic phase with different extractant concentrations, the samples were prepared as follows: 20 mL of the lean organic phase was added into each conical flask containing 20 mL of the aqueous feed and kept in the thermostated water bath (Techne Te-1D, Techne Co., UK) at (25.0±0.01) °C, and then stirred with a magnetic stirrer outside the water bath for 20 min. The two phases were rapidly transferred into a 60 mL separatory funnel, followed by phase separation to obtain the loaded organic phase and the aqueous raffinate. Then, the loaded organic phase was centrifuged (3000 r/min, 5 min) to remove any residual water. The aqueous feed was the same aqueous solution as mentioned in Section 2.2. The concentrations of the lean organic phases containing HDNNS and 4PC ranged from 1×10^{-7} to 0.45 mol/L.

2.5 Small angle X-ray scattering (SAXS) measurements

SAXS patterns were recorded on a SAXSess system (Anton-Paar, Austria) with a Cu K_{α} radiation (0.1542 nm) operating at 50 kV and 40 mA [26]. Samples were introduced into a quartz capillary and placed inside an evacuated chamber. The distance between the sample and the detector was around 259.2 mm. The data acquisition time was 30 min for each sample. Except as noted, the temperature was kept at (25.0±0.1) °C. The 2D scattering patterns were recorded by an imaging-plate (IP) detector (a Cyclone, PerkinElmer) and integrated into 1D scattered intensity (q) as a function of the magnitude of the scattering vector $q = (4\pi/\lambda)\sin(\theta/2)$ using SAXS Quant software (Anton Paar), where θ and λ are the total scattering angle and the wavelength of the incident beam, respectively. All $I(q)$ data were corrected for the background scattering from the capillary and the solvents. The background scattering (solvent-filled capillary) was measured separately and subtracted from the scattering curves. The collected data were radially averaged and

normalized to the intensity of the transmitted beam.

In the present study, SAXS data were interpreted by the GIFT method [27] to obtain pair-distance distribution functions (PDDFs: structure information in real space), and provide information on the shape and the size of the particles in real space without making any assumption.

The scattering intensity $I(q)$ for monodisperse, homogeneous, and spherical particle is generally described by

$$I(q) = NP(q)S(q) \quad (2)$$

where N is the total number of particles, and $P(q)$ and $S(q)$ are the form and structure factors, which correspond to the shape and size of the scattering particle and the interparticle interactions, respectively. In the polydisperse system, $P(q)$ and $S(q)$ are averaged form factor and structure factor, respectively.

By the Fourier transformation of PDDFs, $P(q)$ is defined as

$$P(q) = 4 \int_0^{\infty} p(r) \frac{\sin(qr)}{qr} dr \quad (3)$$

Since the structure of reverse micelles was deduced from $p(r)$, the inverse Fourier transformation of $P(q)$ must be calculated. An interaction potential model for $S(q)$ must be involved, where we chose the averaged structure factor model of hard sphere [28] in the current study and Percus–Yevick closure relation [29] to solve the Ornstein–Zernicke equation. A detailed description on the treatment of SAXS data using GIFT is given by FRITZ and GLATTER [30]. In the current study, the loaded organic phases after phase separation tests as mentioned in Section 2.4 were taken for SAXS measurements.

3 Results and discussion

3.1 Specific settling rates of Co(II) and blank systems

The results of the phase separation rate for the Co(II) system and blank systems are shown in Fig. 2, where the specific settling rates (SSR) are plotted versus the concentration of extractant. For the Co(II) system, it is notable that the values of the SSR are apparently decreased from 3.2 to 1.72 $\text{m}^3/(\text{m}^2 \cdot \text{h})$ when the concentration of the extractant increases from 0.1 to 0.45 mol/L. For the blank system, the values of the SSR show a slight decrease from 0.90 to 0.47 $\text{m}^3/(\text{m}^2 \cdot \text{h})$ with the increase of the extractant concentration from 0.1 to 0.45 mol/L. The values of the SSR in the Co(II) system are much higher than those in the blank system at the same extractant concentration.

There are some differences in the trend of the phase separation rate between the two systems with the concentration of extractant increasing. As mentioned by

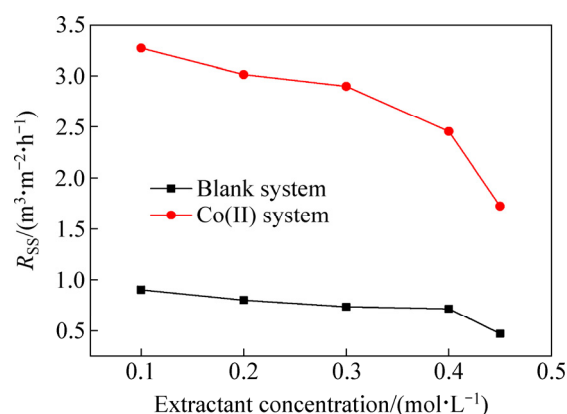


Fig. 2 Effect of extractant concentrations on phase separation of Co(II) and blank systems

other researchers [12,31], the correlations based on some physical properties such as viscosity, density and interfacial tension are superior to estimate or roughly predict the phase separation behavior for solvent extraction. So, it is necessary to identify the physicochemical parameter(s) responsible for the different phase separation behavior in the Co(II) and blank systems.

3.2 Physicochemical properties

The interfacial tensions between the loaded organic phases and the aqueous raffines are listed in Table 1. For the Co(II) system, it is obvious that there is no significant variation in interfacial tension values ((5.49 ± 0.64) mN/m) with the increase of the extractant concentration from 0.1 to 0.45 mol/L, and similar result ((4.97 ± 0.37) mN/m) and trend exist in the blank system. This behavior could be explained by the increasing adsorption of the extractant molecules at the liquid–liquid interface. In general, the higher the interfacial tension values, the faster the phase separations between organic and aqueous phases in hydro-metallurgical operations [32,33]. However, the specific settling rates (SSR) of the blank system decrease slightly with the increase of the extractant concentration, and those of the Co(II) system are decreased apparently (Fig. 2). These results suggest that there are factors other

Table 1 Interfacial tensions for Co(II) and blank systems

Extractant concentration/(mol·L ⁻¹)	Interfacial tension/(mN·m ⁻¹)	
	Co(II) system	Blank system
0.1	4.85	5.34
0.2	5.80	5.25
0.3	6.13	5
0.4	6.09	4.6
0.45	6.08	5.31

than interfacial tension which influence apparently the phase separation rate.

The effects of densities of the loaded organic phases and the aqueous raffinate on the phase separation behavior of the Co(II) and blank systems are listed in Tables 2 and 3, respectively. The density of the aqueous raffinate has almost no change with the increase of the extractant concentration in both the Co(II) and blank systems. As for the Co(II) system (in Table 2), with the increase of the extractant concentration, the densities of the loaded organic phases are ranged from 0.805 to 0.888 g/cm³. As for the blank system (in Table 3), the densities of the loaded organic phases are ranged from 0.808 to 0.890 g/cm³ when the extractant concentration increases from 0.1 to 0.45 mol/L. It is evident that the densities of the loaded organic phases are comparable for the Co(II) and the blank systems, which suggests that the density of the two phases is not a major factor affecting the performance of the phase separation. Similar results were reported by PATHAK et al [12] and GONG [34].

Table 2 Densities of loaded organic phases and aqueous raffinate for Co(II) system

Extractant concentration/(mol·L ⁻¹)	Density/(g·cm ⁻³)	
	Loaded organic phases	Aqueous raffinate
0.1	0.805	1.075
0.2	0.832	1.074
0.3	0.848	1.073
0.4	0.869	1.072
0.45	0.888	1.071

Table 3 Densities of loaded organic phases and aqueous raffinate for blank system

Extractant concentration/(mol·L ⁻¹)	Density/(g·cm ⁻³)	
	Loaded organic phases	Aqueous raffinate
0.1	0.808	1.061
0.2	0.832	1.061
0.3	0.855	1.060
0.4	0.879	1.061
0.45	0.890	1.059

Apart from density and interfacial tension, other factors such as the viscosity of the loaded organic phase need to be taken into account for obtaining a good understanding of the phase separation behavior. The effect of the viscosity of the loaded organic phase on the phase separation was studied for the Co(II) and blank system, and the results are shown in Fig. 3. It can be seen that with the increase of the extractant concentration

from 0.1 to 0.45 mol/L, the viscosity values of the loaded organic phases for the Co(II) system increase from 1.909 to 7.935 mPa·s, and those for the blank system increase from 1.949 to 8.482 mPa·s. It is particularly noteworthy that the extent of the increase of the viscosity of the loaded organic phase for the Co(II) system is less than that for the blank system. Combined with the results in Fig. 2, we can conclude that the increase of the viscosity of the loaded organic phase decelerates the phase separation rate for the Co(II) system and blank system.

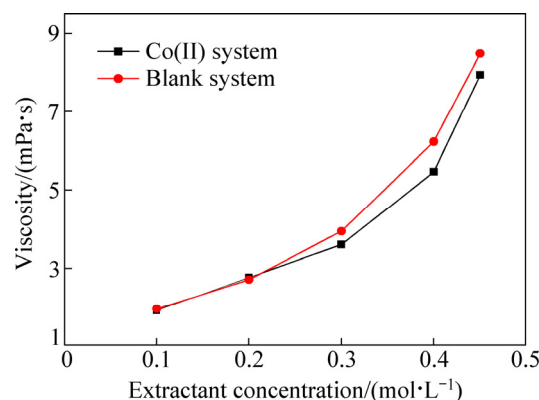


Fig. 3 Change of viscosity of loaded organic phase with extractant concentration

ALBERTS and DORFLING [35], and MUSADAIDZWA and TSHININGAYAMWE [36] supposed that an increase in the viscosity of the loaded organic phases results in the difficulty of the phase separation. TESTARD et al [37] speculated that the higher viscosity of the loaded organic phase is a direct consequence of the elongation of the aggregates when cations are extracted. However, no experiments have been conducted to confirm this idea in the literature.

The results of interfacial tension between the loaded organic phase and the aqueous raffinate varying with extractant concentration are shown in Fig. 4. The critical micelle concentration (CMC) of the loaded organic phase

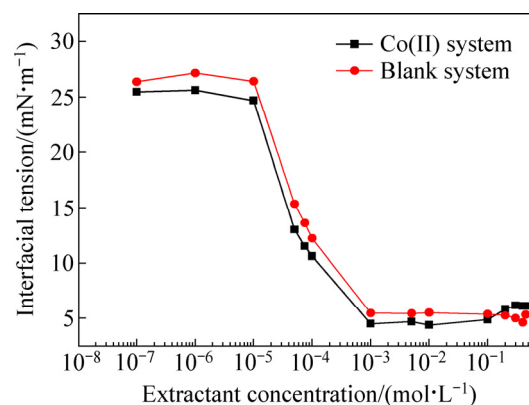


Fig. 4 Variation of interfacial tension with extractant concentration

can be determined to be about 1×10^{-3} mol/L for both the blank and Co(II) systems. This result is somewhat higher than the CMC of pure HDNNS [38,39]. However, the extractant concentration of the loaded organic phases in Fig. 2 (0.1–0.45 mol/L) is much higher than the CMC of the loaded organic phases from Fig. 4. That is to say, the reverse micelles in the loaded organic phase are formed when the extractant concentrations range from 0.1 to 0.45 mol/L.

3.3 Water uptake and small angle X-ray scattering (SAXS) results

Although the reversed micelles can form in the loaded organic phases, the water pool in their core is often taken to be as quite a distinctive characteristic of reversed micelles [40]. The total water uptake and the metal concentration in the loaded organic phase for the Co(II) system are listed in Table 4. From Table 4, it can be seen that the change of the metal concentration in the loaded organic phase has the same order of magnitude for the Co(II) systems, and that the total water uptake of the loaded organic phase in the blank system is more than that in the Co(II) system.

Table 4 Total water uptake and metal concentration in loaded organic phase

Extractant concentration/ (mol·L ⁻¹)	Co(II) system		Blank system
	Total water uptake/ (mol·L ⁻¹)	[Co]/ (mol·L ⁻¹)	Total water uptake/ (mol·L ⁻¹)
0.1	0.325	0.008	0.345
0.2	0.642	0.020	0.709
0.3	0.937	0.025	1.084
0.4	1.235	0.035	1.478
0.45	1.409	0.042	1.703

According to our previous work [23], the coordination structure of the extracted Co(II) complex, $\text{Co}(\text{H}_2\text{O})_4(\text{4PC})_2(\text{DNNS})_2$, existed in the loaded organic phase of the Co(II) system. It is speculated that the excess water uptake beyond the corresponding metal-to-water molar ratios of 1:4 in the extracted metal complexes indicates a change in the loaded organic phases for the Co(II) systems. We can deduce that the excess water uptake results from the water solubilization into the water pool of the reverse micelles in the loaded organic phase. This opinion is also supported by other researchers [41,42]. As for the blank system, there are no extracted metal complexes in the loaded organic phases, therefore there is no metal ion and water to be coordinated, so the total water uptake in the loaded organic phase is the solubilized water (the excess water uptake) in the micelles.

The excess water uptake (c_2 , mol/L) in the water pool of the reversed micelles can be calculated as follows:

$$c_1 = n \cdot c_0 \quad (4)$$

$$c_2 = c_T - c_1 \quad (5)$$

where c_T (mol/L), c_0 (mol/L), c_1 (mol/L) and n are the total water uptake, the metal concentration of the loaded organic phase, the concentration of the coordinated water and the number of coordinated water molecules in the loaded organic phases ($n=4$ for the Co(II) system), respectively.

The values of the excess water uptake for the Co(II) system are summarized in Table 5. It can be found that the values of the excess water uptake in the water pool of the reversed micelles increase with the increase of the extractant concentration for the Co(II) system. Combined with the results in Table 4, the excess water uptake (the total water uptake) in the blank system is much higher than that in the Co(II) system. For example, when the extractant concentration is 0.45 mol/L, the values of the excess water uptake are 1.241 and 1.70 mol/L for the Co(II) and blank systems, respectively.

Table 5 Excess water uptake in loaded organic phases

Extractant concentration/(mol·L ⁻¹)	c_1 /(mol·L ⁻¹)	c_2 /(mol·L ⁻¹)
0.1	0.032	0.293
0.2	0.08	0.562
0.3	0.1	0.837
0.4	0.14	1.095
0.45	0.168	1.241

From the above-mentioned results, we can assume that for the Co(II) and blank system, with the significant increase of the excess water uptake in the loaded organic phase, the size of the reverse micelles (1–20 nm [43]) increases dramatically, which may result in the formation of reverse microemulsion (10–100 nm [44]) or reverse vesicles (>100 nm [45]). And the increase of the viscosity in the loaded organic phase (shown in Fig. 3) could be attributed to the dramatic growth of the size of the reversed micelles, which may lead to the significant deceleration of the phase separation in solvent extraction. Meanwhile, when the concentration of the extractant is the same for both the blank and Co(II) systems, the total water uptake of the blank system is much more than that of the Co(II) system (listed in Tables 4 and 5), and the size growth of the reverse micelles in the blank system may increase much more than that in the Co(II) system. Moreover, as shown in Fig. 3, the viscosity of the loaded organic phase for the blank system is higher than that for the Co(II) system, which may result in more apparent

deceleration of the specific settling rates for the blank system than that for the Co(II) system at the same extractant concentrations.

SAXS experiments were performed to investigate the morphology of the species of the loaded organic phases in the whole range of extractant concentrations (0.1–0.45 mol/L). The SAXS original curves of the loaded organic phases in n-dodecane at different extractant concentrations and the corresponding PDDFs are shown in Fig. 5. As shown in Figs. 5(a) and 5(b), the main difference between these waves comes from the low- q range, which is more sloped in the low concentration case. A qualitative description of the morphology of these samples may be indicated by power law behavior in the low- q region of the SAXS data, where a slope of -1 and 0 on the log–log scale suggests the development of rod-like aggregates and spherical aggregates, respectively [46,47]. These SAXS original curves suggest (Figs. 5(a) and 5(b)) that the reverse micelles may undergo a transition from rod-like to spherical reverse micelles.

Information about the morphology of the reversed micelles in the loaded organic phases comes from the GIFT-generated $p(r)$ functions named PDDF for the SAXS original curves, which describes the scattering entity by a distribution of distances between points

within the assembly, with r being the distance and $p(r)$ being the relative number of the particular distances that occur. As shown in Figs. 5(c) and 5(d), the value of r at which $p(r)$ becomes zero estimates the maximum length of the reverse micelles (D_{\max}). For the Co(II) system (Fig. 5(c)), a one-dimensional growth of aggregates (D_{\max}) extends from 3.6 to 4.0 nm in length with a constant cross-sectional radius of nearly 1.5 nm, which is calculated by the PDDFs of the SAXS original curves. These results show that rod-like reversed micelles are formed in the loaded organic phases with the increase of the extractant concentration from 0.1 to 0.2 mol/L. But for the blank system (Fig. 5(d)) with the extractant concentration of 0.1 mol/L, the distribution is asymmetrical, which suggests that reversed micelles with a constant cross-sectional radius of nearly 1.5 nm and D_{\max} of 8 nm form in rod-like shape. But with the increase of the extractant concentration from 0.2 to 0.45 mol/L, the morphology of the reversed micelles turns into spherical shapes.

Therefore, the change of the morphology of the reversed micelles follows the same trend as the change of excess water uptake in the loaded organic phases for the Co(II) system. The results of the SAXS data for Co(II) system show an excellent agreement with our assumption that the dramatic elongation of the morphology of the

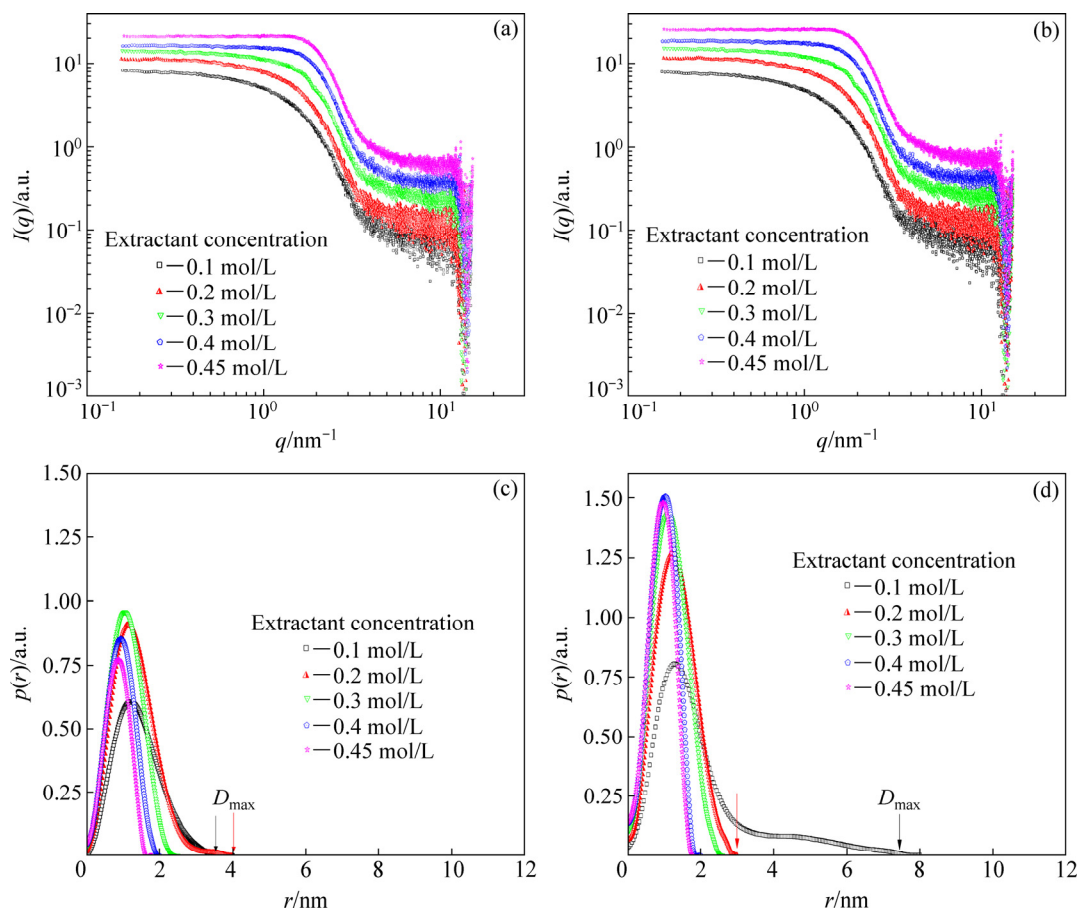


Fig. 5 Background subtracted, normalized SAXS waves (a, b) and PDDFs (c, d) for Co(II) system (a, c) and blank system (b, d)

reversed micelles results in the deceleration of the specific settling rates with the increase of the extractant concentration from 0.1 to 0.2 mol/L.

However, when the extractant concentration increases from 0.3 to 0.45 mol/L for the Co(II) system and from 0.2 to 0.45 mol/L for the blank system, a bell-shaped and symmetrical function in Figs. 5(a) and 5(d) shows that the reversed micelles with an evident spherical shape at a polar core diameter of ~ 1 nm (deduced with the GIFT technique of the SAXS original curves) exist in the loaded organic phases for both the blank and Co(II) systems. The morphology of the reversed micelles undergoes a structural transition from rod-like to spherical reversed micelles, which is not in accordance with our above-mentioned assumption (the morphology of the reversed micelles should be elongated to several nanometers or even to a few micrometers). The abnormal phenomenon could be resulted from the SAXS equipment itself. On one hand, the SAXS equipment we used may not be suitable for the measurement of the morphology (size and shape) of the reversed micelles in the loaded organic phase with higher extractant concentrations, because the morphology of oil-in-water micelles with lower concentrations of surfactants is often investigated by the present SAXS equipment [48]. On the other hand, it should be noted that the maximum length of the reverse micelles, D_{\max} , depends on the maximum of resolution (or q_{\min}) of the measurement, and q_{\min} in the present equipment equals $\sim 0.1 \text{ nm}^{-1}$. Moreover, D_{\max} as determined by the GIFT method shown in $p(r)$ functions may not be the actual length of the reverse micelles (the actual length of reverse micelles with much higher extractant concentration may be of hundreds of nanometers to a few micrometers), because we do not have the scattering behavior below $q_{\min} \approx 0.1 \text{ nm}^{-1}$. Therefore, a SAXS equipment compatible with high-resolution structural studies such as synchrotron based small angle X-ray or neutron scattering (SANS) is needed to give a more intuitive and convincing picture on such a problem.

4 Conclusions

(1) The specific settling rates of the Co(II) and blank systems decrease with the increase of the extractant concentration from 0.1 to 0.45 mol/L. With the increase of the extractant concentrations, the interfacial tension and the difference in density of the two phases are nearly unchanged.

(2) The viscosity and the total water uptake of the loaded organic phase in the blank system are higher than those in the Co(II) system within the extractant concentration range studied. The extractant concentration of the loaded organic phase is much higher than the

CMC (1×10^{-3} mol/L), and the formation of the reversed micelles in the loaded organic phase occurs when the extractant concentrations range from 0.1 to 0.45 mol/L. It can be concluded that the deceleration of the specific settling rates with increasing extractant concentrations under the current test conditions may be due to the tremendous increase of the viscosity and the water uptake or in a microscopic view, the change of morphology (size and shape) of the reversed micelles.

(3) The SAXS results show a one-dimensional growth of aggregates from 3.6 to 4.0 nm in length with a constant cross-sectional radius of nearly 1.5 nm when the extractant concentration ranges from 0.1 to 0.2 mol/L for the Co(II) system. As for the blank system, the reversed micelles with a constant cross-sectional radius of nearly 1.5 nm undergo elongation and evolve into rod-like shape with 8 nm in length at the extractant concentration of 0.1 mol/L. However, when extractant concentration is correspondingly beyond 0.2 mol/L for the blank system and beyond 0.3 mol/L for the Co(II) system, a turning point occurs, and the shape of reversed micelles changes into spherical with a polar core diameter of ~ 1 nm, not a more elongated structure for the lack of a SAXS equipment compatible with high-resolution structural studies such as synchrotron based small angle X-ray or neutron scattering (SANS).

Acknowledgments

The authors thank ExxonMobil Chemical for kindly supplying the Escaid 110.

References

- [1] FLETT D S. New reagents or new ways with old reagents [J]. *Journal of Chemical Technology & Biotechnology*, 1999, 74(2): 99–105.
- [2] CHENG Chu-yong, BARNARD K R, ZHANG Wen-sheng, ROBINSON D J. Synergistic solvent extraction of nickel and cobalt: A review of recent developments [J]. *Solvent Extraction and Ion Exchange*, 2011, 29(5–6): 719–754.
- [3] PRESTON J S, du PREEZ A C. Solvent extraction of nickel from acidic solutions using synergistic mixtures containing pyridinecarboxylate esters. Part 3. Systems based on arylsulphonic acids [J]. *Journal of Chemical Technology & Biotechnology*, 1998, 71(1): 43–50.
- [4] PADILLA R, RUIZ M C, TRUJILLO W. Separation of liquid–liquid dispersions in a deep-layer gravity settler: Part I. Experimental study of the separation process [J]. *Hydrometallurgy*, 1996, 42(2): 267–279.
- [5] HU Fang, HU Hui-ping, HU Jiu-gang, ZHU Shan, YANG Jin-peng, WANG Yon-xi. Improving selective separation of Cu(II) from acidic polymetallic media with 2-ethylhexyl 4-pyridinecarboxylate ester: Extraction behaviors, coordination structure and microscopic mechanism [J]. *Journal of Molecular Liquids*, 2017, 248: 1050–1058.
- [6] LI Ji-yuan. Study on the extraction and mechanism of nickel in polymetallic solution by HDNNS/4PC [D]. Changsha: Central South University, 2017. (in Chinese)

- [7] SUN Zhuo, PAN Yun-cong, JIANG Ji-mu. Design manual for heavy non-ferrous metal smelting (copper-nickel volume) [M]. Beijing: Metallurgical Industry Press, 1996. (in Chinese)
- [8] COUGHLIN R W, BERG R L V. Mass and heat transfer to drops in a mixer-settler [J]. *Chemical Engineering Science*, 1966, 21(1): 3–18.
- [9] WANG Shu-chan, ZHANG Ting-an, ZHANG Zi-mu, LV Chao, ZHAO Qiu-yue, LIU Yan. Effect of stirring on oil-water separation in rare earth mixer-settler [J]. *China Petroleum Processing & Petrochemical Technology*, 2014, 16(3): 99–103.
- [10] EL-RIFAI M A. Composition dynamics in multi-mixer-settler extractive reaction batteries [J]. *Chemical Engineering Science*, 1975, 30(1): 79–87.
- [11] RYON A D, DALEY F L, LOWRIE R S. Design and scale up of mixer-settlers for the DAPEX solvent extraction process [R]. Dapex Process, 1960.
- [12] PATHAK P N, KANEKAR A S, PRABHU D R, MANCHANDA V K. Comparison of hydrometallurgical parameters of N,N-dialkylamides and of tri-n-butylphosphate [J]. *Solvent Extraction & Ion Exchange*, 2009, 27(5–6): 683–694.
- [13] LIU Xiao-rong, QIU Guan-zhou, HU Yue-hua, YANG Jun-he, JIN Min-lin. Effect of Lix984N content on phase disengagement dynamics in copper-SX [J]. *Transactions of Nonferrous Metals Society of China*, 2003, 13(4): 963–967.
- [14] LIU Yan-jun, LIU Xiao-rong, LI Hui, LI Qing, LI Yong-sheng, SU Chang, TIAN Jun, WANG Yu-cheng. Effects of strong-acid on performances of copper solvent extraction [J]. *Advanced Materials Research*, 2014, 881–883: 48–51.
- [15] ASENJO J A, MISTRY S L, ANDREWS B A, MERCHUK J C. Phase separation rates of aqueous two-phase systems: Correlation with system properties [J]. *Biotechnology & Bioengineering*, 2010, 79(2): 217–223.
- [16] XUE Shu-yun, FU Xun, XIONG Ya-hong, ZHANG Shao-na, HU Zheng-shui. Study on the thiophosphinic extractants. I. The basic properties of the extractants and the phase behavior in their saponified systems [J]. *Solvent Extraction and Ion Exchange*, 2002, 20(3): 331–344.
- [17] MOVER B A, McDOWELL W J. Factors influencing phase disengagement rates in solvent extraction systems employing tertiary amine extractants [J]. *Separation Science*, 1981, 16(9): 1261–1289.
- [18] NAKAMURA T, TERASHIMA H, MUKAI K. Emulsion formation and phase separation in some organic solvent-water systems [J]. *Shigen-to-Sozai*, 1992, 108(11): 812–816.
- [19] BAILEY N T, MAHI P. The effect of diluents on the metal extracted and phase separation in the extraction of aluminium with monononyl phosphoric acid [J]. *Hydrometallurgy*, 1987, 18: 351–365.
- [20] RAATZ S, KLAPPER P, REPKE J U. Micellar extraction of zinc using di(2-ethylhexyl)phosphorsure in presence of surfactant cetyltrimethyl ammonium bromide [J]. *Chemie Ingenieur Technik*, 2011, 83(4): 518–524. (in German)
- [21] BARNEA E. Liquid-liquid contacting-art or science? Part I. Characterization of liquid-liquid system [J]. *Hydrometallurgy*, 1979, 5: 15–28.
- [22] ZHU Shan, HU Hui-ping, HU Jiu-gang, LI Ji-yuan, HU Fang, WANG Yong-xi. Structural insights into the extraction mechanism of cobalt(II) with dinonylnaphthalene sulfonic acid and 2-ethylhexyl 4-pyridinecarboxylate ester [J]. *Journal of coordination chemistry*, 2018, 71(15): 2441–2456.
- [23] LI Ji-yuan, HU Hui-ping, ZHU Shan, HU Fang, WANG Yong-xi. The coordination structure of the extracted nickel(II) complex with a synergistic mixture containing dinonylnaphthalene sulfonic acid and 2-ethylhexyl 4-pyridinecarboxylate ester [J]. *Dalton Transactions*, 2017, 46: 1075–1082.
- [24] PRESTON J, PREEZ A D. The solvent extraction of nickel and cobalt by mixtures of carboxylic acids and pyridinecarboxylate esters [J]. *Solvent Extraction & Ion Exchange*, 1995, 13(3): 465–494.
- [25] CHENG C Y, BARNARD K R, DAVIES M G. A study on the chemical stability of the Versatic 10-Acorga CLX50 synergistic system [J]. *Minerals Engineering*, 2002, 15(12): 1151–1161.
- [26] ZHOU Li-ping, ZENG Xiao-qin, LI De-jiang, YANG Chun-ming. Ageing precipitation behavior of Mg–12Gd alloy [J]. *Chinese Journal of Nonferrous Metals*, 2015, 25(6): 1409–1416. (in Chinese)
- [27] FRITZ G, BERGMANN A, GLATTER O. Evaluation of small-angle scattering data of charged particles using the generalized indirect Fourier transformation technique [J]. *Journal of Chemical Physics*, 2000, 113(21): 9733–9740.
- [28] SALGI P, RAJAGOPALAN R. Polydispersity in colloids: Implications to static structure and scattering [J]. *Advances in Colloid & Interface Science*, 1993, 43(2–3): 169–288.
- [29] PERCUS J K, YEVICK G J. Analysis of classical statistical mechanics by means of collective coordinates [J]. *Physical Review*, 1958, 110: 1–13.
- [30] FRITZ G, GLATTER O. Structure and interaction in dense colloidal systems: evaluation of scattering data by the generalized indirect Fourier transformation method [J]. *Journal of Physics Condensed Matter*, 2006, 18(36): S2403–S2419.
- [31] NING Peng-ge, CAO Hong-bin, ZHANG Yi. Stability of the interfacial crud produced during the extraction of vanadium and chromium [J]. *Hydrometallurgy*, 2013, 133(2): 156–160.
- [32] VIDYALAKSHMI V, SUBRAMANIAN M S, RAJESWARI S, SRINIVASAN T G, VASUDEVA RAO P R. Interfacial tension studies of N,N-dialkyl amides [J]. *Solvent Extraction & Ion Exchange*, 2003, 21(3): 399–412.
- [33] RYDBERG J, COX M, MUSIKAS C, CHOPPIN G R. Solvent extraction principles and practice [M]. 2nd ed. Boca Raton: CRC Press, 2004.
- [34] GONG Xing-chu, LV Yang-cheng, LI Mu, MA Xue-feng, NI Qian-yin, LUO Guang-sheng. Selection and evaluation of a new extractant for caprolactam extraction [J]. *Chinese Journal of Chemical Engineering*, 2008, 16(6): 876–880.
- [35] ALBERTS E, DORFLING C. Stripping conditions to prevent the accumulation of rare earth elements and iron on the organic phase in the solvent extraction circuit at skorpion zinc [J]. *Minerals Engineering*, 2013, 40(40): 48–55.
- [36] MUSADAIDZWA J M, TSHININGAYAMWE E I. Skorpion zinc solvent extraction: The upset conditions [J]. *Journal of the Southern African Institute of Mining & Metallurgy*, 2009, 109: 691–695.
- [37] TESTARD F, BAUDUIN P, ZEMB T, BERTHON L. Third-phase formation in liquid/liquid extraction: A colloidal approach [M]. Boca Raton, FL and London: CRC Press, Taylor & Francis Group, 2010.
- [38] CHIARIZIA R, DANESI P R, D'ALESSANDRO G, SCUPPAR B. Interfacial behaviour of dinonylnaphthalenesulfonic acid at the toluene–HClO₄ interface [J]. *Journal of Inorganic & Nuclear Chemistry*, 1976, 38(7): 1367–1369.
- [39] OSSEO-ASARE K, KEENEY M E. Aspects of the interfacial chemistry of nickel extraction with LIX63-HDNNS mixtures [J]. *Metallurgical and Materials Transactions B*, 1980, 11: 63–67.
- [40] WONG M, THOMAS J K, GRAETZEL M. Fluorescence probing of inverted micelles. The state of solubilized water clusters in alkane diisooctyl sulfosuccinate (aerosol ot) solution [J]. *Journal of the American Chemical Society*, 1976, 98(9): 2391–2397.
- [41] LI Quan, WENG Shi-fu, WU Jin-guang, ZHOU Nai-fu. Comparative study on structure of solubilized water in reversed micelles I. FT-IR spectroscopic evidence of water/AOT/n-heptane and water/NaDEHP/n-heptane systems [J]. *Journal of Physical Chemistry B*, 1998, 102(17): 3168–3174.
- [42] ANTONIO M R, CHIARIZIA R, GANNAZ B, BERTHON L, ZORZ N, HILL C, COTE G. Aggregation in solvent extraction systems containing a malonamide, a dialkylphosphoric acid and their

- mixtures [J]. Separation Science & Technology, 2008, 43(9–10): 2572–2605.
- [43] LAW S J, BRITTON M M. Sizing of reverse micelles in microemulsions using NMR measurements of diffusion [J]. Langmuir, 2012, 28(32): 11699–11706.
- [44] SHINODA K, FRIBERG S. Microemulsions: colloidal aspects [J]. Advances in Colloid & Interface Science, 1975, 4(4): 281–300.
- [45] KUNIEDA H, SHIGETA K, NAKAMURA K, IMAE T. Formation and structure of reverse vesicles [J]. Progress in Colloid & Polymer Science, 1996, 100: 1–5.
- [46] SHARMA S C, SHRESTHA R G, SHRESTHA L K, ARAMAKI K. Viscoelastic wormlike micelles in mixed nonionic fluorocarbon surfactants and structural transition induced by oils [J]. Journal of Physical Chemistry B, 2009, 113(6): 1615–1622.
- [47] SHRESTHA L K, SHRESTHA R G, ARAMAKI K. Intrinsic parameters for the structure control of nonionic reverse micelles in styrene: SAXS and rheometry studies [J]. Langmuir, 2011, 27(10): 5862–5873.
- [48] SHRESTHA L K, SATO T, DULLE M, GLATTER O, ARAMAKI K. Effect of lipophilic tail architecture and solvent engineering on the structure of trehalose-based nonionic surfactant reverse micelles [J]. Journal of Physical Chemistry B, 2010, 114(37): 12008–12017.

采用 HDNNS/4PC 协萃体系从硫酸盐中萃取钴过程中的相分离

黄婷, 王永茜, 胡慧萍, 胡芳, 罗雨晴, 刘士军

中南大学 化学化工学院, 长沙 410083

摘要: 相分离速率是决定溶剂萃取体系在湿法冶金中得到应用的关键。研究二壬基萘磺酸和 4-吡啶甲酸异辛酯协同混合体系从单金属硫酸盐溶液中萃取钴的相分离, 探索负载有机相的物理化学性质以及反胶束的形态对相分离的影响。结果表明, 负载有机相的黏度及增溶水量是影响相分离的主要因素。随着这两个因素的增加, 混合澄清速率明显降低。X 射线小角散射(SAXS)测量结果证实负载有机相中反相胶束的形貌会随混合澄清速率的变化而变化。

关键词: 协同溶剂萃取; 相分离; 混合澄清速率; 反胶束; 钴

(Edited by Bing YANG)